mathematics

Article

Grey-Black Optical Solitons, Homoclinic Breather, Combined Solitons via Chupin Liu's Theorem for Improved Perturbed NLSE with Dual-Power Law Nonlinearity

Syed T. R. Rizvi [1], Aly R. Seadawy [2,*] and Shami A. M. Alsallami [3]

[1] Department of Mathematics, COMSATS University Islamabad, Lahore Campus, Lahore 54840, Pakistan
[2] Mathematics Department, Faculty of Science, Taibah University, Al-Madinah Al-Munawarah 41411, Saudi Arabia
[3] Department of Mathematical Sciences, College of Applied Science, Umm Al-Qura University, Makkah 21955, Saudi Arabia
* Correspondence: aabdelalim@taibahu.edu.sa

Abstract: In this article, we consider the improved perturbed nonlinear Schrödinger Equation (IP-NLSE) with dual power law nonlinearity, which arises in optical fibers and photovoltaic-photo-refractive materials. We found grey and black optical solitons of the governing equation by means of a suitable complex envelope ansatz solution. By using the Chupin Liu's theorem (CLT) for the grey and black solitons, we evaluated new categories of combined optical soliton (COS) solutions to the IP-NLSE. The propagation behaviors for homoclinic breathers (HB), multiwaves and *M*-shape solitons will be analytically examined. All new analytical solutions will be found by an ansatz function scheme and suitable transformations. Multiwave solitons have been reported by using a three-waves technique. Furthermore, two kinds of interactions for *M*-shape soliton through exponential functions will be examined.

Keywords: solitons; IP-NLSE; ansatz functions method; breathers; interaction phenomena

MSC: 35J05; 35J10; 35K05; 35L05

check for updates

Citation: Rizvi, S.T.R.; Seadawy, A.R.; Alsallami, S.A.M. Grey-Black Optical Solitons, Homoclinic Breather, Combined Solitons via Chupin Liu's Theorem for Improved Perturbed NLSE with Dual-Power Law Nonlinearity. *Mathematics* **2023**, *11*, 2122. https://doi.org/10.3390/math11092122

Academic Editors: António Lopes, Omid Nikan and Zakieh Avazzadeh

Received: 1 March 2023
Revised: 31 March 2023
Accepted: 25 April 2023
Published: 30 April 2023

1. Introduction

Optical solitons have been extensively applied in high-speed and high-capacity communication systems as an information carrier. The nonlinear Schrödinger Equation (NLSE) is one of the rarely used models in this context and describes the evolution in optics [1–19]. Recently, the study of exact rational solutions, their interactions, homoclinic breathers and multiwaves has been receiving attention from many scientists for their applications in biophysics, nonlinear fibers, oceanography and plasma. There are some adequate techniques that are applied to achieve the retrieval of rational solutions to the nonlinear systems [20–34].

The IP-NLSE in its dimensionless form is given as [35],

$$i\Omega_t + a\Omega_{tx} + b\Omega_{xx} + cF\left(|\Omega|^2\right)\Omega = i\left(c_3\Omega_x + c_4\left(|\Omega|^{2m}\Omega\right)_x + c_5\left(|\Omega|^{2m}\right)_x\Omega\right) \tag{1}$$

where x and t stand for the spatial and temporal variables, respectively, while $\Omega(x,t)$ is the soliton pulse profile. The 1st term interprets the linear evolution. The m stands for a nonlinearity factor that is applied to put the model into a generalized setting. c_4 represents the self-steepening perturbation term, while the coefficient of c_3 is the inter-modal dispersion and c_5 is the nonlinear dispersion coefficient. The coefficient of b accounts for the group velocity dispersion and the coefficient of a accounts for spatio-temporal dispersion and hence Equation (1) stays integrable. The coefficient c interprets the non-Kerr-law nonlinear term. Now, in order to use the functional F, it is important to consider the smoothness of $F(|\Omega|^2\Omega) : C \to C$. Treating the complex plane C as a two-dimensional linear space R^2 the function $F(|\Omega|^2\Omega)$ is continuously differentiable, so that

$$F\left(|\Omega|^2\right)\Omega \in \bigcup_{n,m=1}^{\infty} C^k\left((-m,m)\times(-n,n) : R^2\right). \tag{2}$$

2. Dual-Power Nonlinearity

This nonlinearity is used in photovoltaic photorefractive materials such as $LiNbO_3$ [35],

$$F(s) = c_1 s^n + c_2 s^{2n} \tag{3}$$

where c_1 and c_2 are constants. Therefore, Equation (1) reduces to [35],

$$i\Omega_t + a\Omega_{tx} + b\Omega_{xx} + \left(c_1|\Omega|^{2n} + c_2|\Omega|^{4n}\right)\Omega = i\left(c_3\Omega_x + c_4\left(|\Omega|^{2m}\Omega\right)_x + c_5\left(|\Omega|^{2m}\right)_x\Omega\right), \tag{4}$$

since for dual power law nonlinearity, $m = n$. Furthermore, as expected, for $n = 1$, the dual power law changes to the parabolic law and Equation (4) will be entertained in the upcoming sections of the paper. Some researchers worked on the stated model. For instance, Biswas et al. investigated optical soliton perturbation via a trial function method [35] and Ekici et al. studied the analysis of solitons in nonlinear materials [36], but the motivation of this document is to find the grey and black optical solitons for the governing equation by means of a suitable complex envelope ansatz solution. With the application of CLT to the grey and black solitons, we evaluate new sets of COS for the model. Furthermore, we will discuss the propagation of homoclinic breathers, multiwaves and rational solitons[37–39].

The rest of the article is as follows: In Section 3, we will give the evaluation of grey and black optical solitons by using a complex envelope ansatz solution. Our Section 4 contains the CLT extended to optical solitons with its applications to the stated model. In Section 5, we will give the evaluation of COS of type-I and in Section 6 the evaluation of COS of type-II. In Section 7, we learn the multiwave solution for the governing problem via a three-waves scheme. In Section 8, the HB scheme is presented and we compute new solitons. In Section 9, we will form the rational solitons and their interactions in Section 10 and Section 11 respectively. Our Section 12, contains the discussions and finally our Section 13 contains the conclusion.

3. Grey and Black Optical Solitons (GBOS)

For these solitons, we apply the following transformation in Equation (4) [40],

$$\Omega(x,t) = B(x,t)e^{i\Xi} \;\; with \;\; \Xi(x,t) = k_2 t - k_1 x + v \tag{5}$$

where the $B(x,t)$ is a complex function, $\Omega(x,t)$ stands for phase shift, v denotes the phase constant, k_2 represents frequency and k_1 represents wave number. To find GBOS for Equation (4), we choose [40]:

$$B(x,t) = \tanh[\eta(x - vt)]\lambda + i\beta \tag{6}$$

where v is pulse width and η denotes inverse group velocity shift. The amplitude of $B(x,t)$ is

$$|B(x,t)| = \left[\lambda^2 + \beta^2 - \lambda^2 \sec h^2(\eta(x - vt))\right]^{\frac{1}{2}} \tag{7}$$

and, furthermore, the nonlinear phase is

$$G_{NL} = \tan^{-1}\left[\frac{\beta}{\lambda\tanh(\eta(x - vt))}\right] \tag{8}$$

For $\beta = 0$ in Equation (6), a dark soliton is known as a black soliton. However, for $\beta \neq 0$ in Equation (6), a GOS is attained.

Substituting Equation (6) into Equation (3):

$$
\begin{aligned}
ic_3k_1\beta + ibk_1^2\beta - ik_2\beta + iak_1k_2\beta - ic_1\beta^3 + ic_4k_1\beta^4 - ic_2\beta^5 - ic_2\tanh^4(\eta)\beta\lambda^4 \\
+\left(-2ic_4k_1\beta^3 - 2ic_5k_1\beta^3\right)\sqrt{\beta^2 + \tanh^2(\eta)\lambda^2} + \left(-ic_1\beta\lambda^2 + ic_4k_1\beta\lambda^2 - 2ic_2\beta^3\lambda^2\right)\tanh^2(\eta) + \\
\left(-c_3k_1\lambda - bk_1^2\lambda + k_2\lambda - ak_1k_2\lambda + c_1\beta^2\lambda - c_4\beta^4\lambda + c_1\lambda\right) + \\
\left(6c_4k_1\beta^2\lambda + 6c_5k_1\beta^3\lambda\right)\sqrt{\beta^2 + \tanh^2(\eta)\lambda^2}\tanh(\eta) + \\
c_2\lambda^5\tanh^4(\eta) + \left(-c_4k_1\lambda^3 + 2c_2\beta^2\lambda^3\right) - c_1\lambda^3\sec h^2(\eta)\tanh(\eta) \\
+\left(6ic_4k_1\beta\lambda^2 + 6ic_5\beta\lambda^2\right)\tan h^2(\eta)\sqrt{\beta^2 + \tan h^2(\eta)\lambda^2} + \\
\left(-2c_4k_1\lambda^3 - 2c_5k_1\lambda^3\right)\tan h^3(\eta)\sqrt{\beta^2 + \tan h^2(\eta)\lambda^2} = 0
\end{aligned}
\tag{9}
$$

Solving distinct equations from the coefficients of tanh, tanh $\tanh^2$ and $\tanh^2$ we find the following:

Constants:

$$ic_3k_1\beta + ibk_1^2\beta - ik_2\beta + iak_1k_2\beta - ic_1\beta^3 + ic_4k_1\beta^4 - ic_2\beta^5 = 0, \tag{10}$$

$\tanh^2$:

$$-ic_1\beta\lambda^2 + ic_4k_1\beta\lambda^2 - 2ic_2\beta^3\lambda^2 = 0, \tag{11}$$

$\sqrt{\beta^2 + \tanh^2(\eta)\lambda^2}$:

$$-2ic_4k_1\beta^3 - 2ic_5k_1\beta^3 = 0, \tag{12}$$

$\sqrt{\beta^2 + \tanh^2(\eta)\lambda^2}\tanh(\eta)$:

$$6c_4k_1\beta^2\lambda + 6c_5k_1\beta^3\lambda = 0, \tag{13}$$

$\tanh(\eta)$:

$$-c_3k_1\lambda - bk_1^2\lambda + k_2\lambda - ak_1k_2\lambda + c_1\beta^2\lambda - c_4\beta^4\lambda + c_1\lambda = 0, \tag{14}$$

$\sqrt{\beta^2 + \tanh^2(\eta)\lambda^2}\tanh(\eta)^2$:

$$6ic_4k_1\beta\lambda^2 + 6ic_5\beta\lambda^2 = 0, \tag{15}$$

$\tanh(\eta)^3$:

$$-2c_4k_1\lambda^3 - 2c_5k_1\lambda^3 = 0 \tag{16}$$

3.1. Type 1: Grey Optical Soliton (GOS) ($\beta \neq 0$)

By evaluation of equations from Equation (10) to Equation (15) for $\beta \neq = 0$, we get [40]:

$$
\begin{cases}
k_1 = \frac{2c_2\beta^2}{c_4}, \\
k_2 = -\frac{c_2\beta^2\left(4b\beta^2c_2 + \beta^2c_4^2 + 2c_3c_4\right)}{c_4(2a\beta^2c_2 - c_4)}, \\
c_5 = -c_4, \\
\lambda = \lambda, \\
\beta = \beta.
\end{cases}
\tag{17}
$$

Hence, the GOS of Equation (3) is

$$\Omega_1(x,t) = \exp\left[i\left(v - \frac{2c_2x\beta^2}{c_4} + -\frac{c_2\beta^2\left(4b\beta^2c_2 + \beta^2c_4^2 + 2c_3c_4\right)t}{c_4(2a\beta^2c_2 - c_4)}\right)\right](-i\beta + \lambda\tanh(\eta)). \tag{18}$$

The pulse intensity is

$$|\Omega_1(x,t)| = \left\{\beta^2 + \lambda^2 - \lambda^2\sec h^2[\eta(x - vt)]\right\}^{\frac{1}{2}}. \tag{19}$$

The nonlinear phase shift is

$$\Omega_{1NL} = \arctan\left[\frac{\beta}{\lambda\tan h[\eta(x - vt)]}\right]. \tag{20}$$

The soliton will exist provided $\eta > 0$ and $v > 0$.

3.2. Type 2: Black Optical Soliton (BOS) ($\beta = 0$)

By evaluation of equations from Equation (10) to Equation (15) for $\beta = 0$, we get [40]:

$$\begin{cases} k_2 = -\frac{bk_1^2 - c_1\lambda^2 + c_3k_1}{ak_1 - 1}, \\ c_5 = -c_4, \\ v = v, \\ \beta = \beta, \\ \lambda = \lambda. \end{cases} \tag{21}$$

Hence, the black optical soliton of Equation (3) is

$$\Omega_2(x,t) = \lambda\exp\left[i\left(v - k_1x + \frac{\left(bk_1^2 - c_1\lambda^2 + c_3k_1\right)t}{ak_1 - 1}\right)\right]\tanh(\eta). \tag{22}$$

Its intensity is

$$|\Omega_2(x,t)| = \left\{\lambda^2 - \lambda^2\sec h^2[\eta(x - vt)]\right\}^{\frac{1}{2}}. \tag{23}$$

4. Optical Solitons Extension via Chupin Liu's Theorem (CLT)

The CLT shows a relationship among kink–bell and kink-type solutions [40]. This theorem is also used for nonlinear fibre optics. This theorem can be used to compute the COS results of a nonlinear model. For this reason, we will utilize the CLT to extract the COS of governing model via the GOS and BOS Equations (18) and (22). Hence, the modified Chupin Liu's Theorem on the relationship among dark–bright and dark soliton solutions is given by the subsequent definition. Suppose we are given a nonlinear model,

$$\begin{cases} \Delta_1(\Omega, \Lambda, \Omega_x, \Lambda_x, \Omega_t, \Lambda_t, \Omega_{xx}, \Lambda_{xx}, \ldots) = 0, \\ \Delta_2(\Omega, \Lambda, \Omega_x, \Lambda_x, \Omega_t, \Lambda_t, \Omega_{xx}, \Lambda_{xx}, \ldots) = 0. \end{cases} \tag{24}$$

Here, $\Omega = \Omega(x,t)$, $\Lambda = \Lambda(x,t)$, Δ_1 and Δ_2 are polynomials about Ω, Λ and their derivatives. If Equation (24) has dark soliton solutions

$$\begin{cases} \Omega = G_k\{\tanh[B(x - vt + \varsigma_0)]\}, \\ \Lambda = H_m\{\tanh[B(x - vt + \varsigma_0)]\}. \end{cases} \tag{25}$$

then Equation (24) has COS

$$\begin{cases} \Omega = G_k\{\tanh[2B(x - vt + \varsigma_0)] + i\text{sech}[2B(x - vt + \varsigma_0)]\}, \\ \Lambda = H_m\{\tanh[2B(x - vt + \varsigma_0)] + i\text{sech}[2B(x - vt + \varsigma_0)]\}. \end{cases} \tag{26}$$

where G_k and H_m are polynomials.

5. COS Category-I

By using the CLT to the GOS Equation (18), we derive the following COS of category-I,

$$\Omega_3(x,t) = \exp\left[i\left(v - \frac{2c_2 x\beta^2}{c_4} + -\frac{c_2\beta^2\left(4b\beta^2 c_2 + \beta^2 c_4^2 + 2c_3 c_4\right)t}{c_4(2a\beta^2 c_2 - c_4)}\right)\right](-i\beta + \lambda\tanh(\eta) + i\sec h(\eta)) \tag{27}$$

with intensity

$$|\Omega_1(x,t)| = \left\{\lambda^2 + \beta^2 + 2\lambda\beta\sec h[2\eta(x - vt)]\right\}^{\frac{1}{2}} \tag{28}$$

and nonlinear phase shift

$$\Omega_{2NL} = \arctan\left[\frac{\beta + \lambda\sec h[2\eta(x - vt)]}{\lambda\tan h[2\eta(x - vt)]}\right] \tag{29}$$

6. COS Category-II

With the application of CLT to the BOS in Equation (22), we compute the COS of category-II:

$$\Omega_4(x,t) = \lambda(\tanh(\eta) + i\text{sech}(\eta))\exp\left[i\left(v - k_1 x + \frac{(bk_1^2 - c_1\lambda^2 + c_3 k_1)t}{ak_1 - 1}\right)\right] \tag{30}$$

with intensity

$$|\Omega_4(x,t)|^2 = \lambda \tag{31}$$

and nonlinear phase shift

$$\Omega_{3NL} = \arctan\left[\frac{\sec h[2\eta(x - vt)]}{\tan h[2\eta(x - vt)]}\right] \tag{32}$$

7. Multiwaves Solitons

The ansatz is [41]:

$$\Omega(x,t) = \psi(\zeta)e^{i\theta}, \;\; \zeta = k_1 x - vt, \;\; \theta = k_2 x - vt. \tag{33}$$

By substituting Equation (33) into Equation (3) and extracting real and imaginary parts respectively:

$$c_3 k_2\psi - bk_2^2\psi + v\psi + ak_2 v\psi + c_1\psi^3 + 3c_4 k_2\psi^3 + 2c_5 k_2\psi^4 + c_2\psi^5 + bk_1^2\psi'' - ak_1 v\psi'' = 0, \tag{34}$$

and

$$c_3 k_1\psi' - 2bk_2 k_1\psi' + v\psi' + ak_1 v\psi' + ak_2 v\psi' + c_4 k_1\psi^2\psi' + 2c_4 k_1\psi^3\psi' + 2c_5 k_1\psi^3\psi' = 0. \tag{35}$$

We apply the following logarithmic transformation to Equations (34) and (35):

$$\psi = 2(\ln f)_\zeta, \tag{36}$$

and obtain,

$$c_3k_2f^4f' - bk_2^2f^4f' + vf^4f' + ak_2vf^4f' + 4c_1f^2f'^3 + 2bk_1^2f^2f'^3 + 12c_4k_2f^2f'^3 - 2ak_1vf^2f'^3 + 16c_5k_2ff'^4 + 16c_2f'^5 - 3bk_1^2f^3f'f'' + 3ak_1vf^3f'f'' + bk_1^2f^4f''' - ak_1vf^4f''' = 0. \tag{37}$$

Moreover, the three-waves ansatz [41] is:

$$f = b_0\cosh(a_1\zeta + a_2) + b_1\cos(a_3\zeta + a_4) + b_2\cosh(a_5\zeta + a_6), \tag{38}$$

where a_i are any constants. Substituting Equation (38) into Equation (37) and solving the equations from of cos, sinh and cosh coefficients:

Set I.

$$\begin{cases} k_2 = \frac{av+c_3+\sqrt{a^2v^2+2ac_3v+4bvc_3^2}}{2b}, \\ k_1 = \frac{av}{b}, \\ a_5 = a_5. \end{cases} \tag{39}$$

We have

$$\Omega_5(x,t) = \frac{2e^{i\left(-vt+\frac{\left(av+c_3+\sqrt{a^2v^2+2ac_3v+4bvc_3^2}\right)x}{2b}\right)}\left(-a_3b_1\cos\left[a_4+a_3\left(-vt+\frac{avx}{b}\right)\right]sin\left[a_4+a_3\left(-vt+\frac{avx}{b}\right)\right]+\Pi_1\right)}{b_1\cos\left[a_4+a_3\left(-vt+\frac{avx}{b}\right)\right]+b_0cos\left[a_2+a_1\left(-vt+\frac{avx}{b}\right)\right]+b_2cosh\left[a_6+a_5\left(-vt+\frac{avx}{b}\right)\right]}, \tag{40}$$

where $\Pi_1 = a_1b_0\cos\left[a_2+a_1\left(-vt+\frac{avx}{b}\right)\right]sinh\left[a_2+a_1\left(-vt+\frac{avx}{b}\right)\right]+\Pi_2$,

and $\Pi_2 = a_5b_2\cosh\left[a_6+a_5\left(-vt+\frac{avx}{b}\right)\right]sinh\left[a_6+a_5\left(-vt+\frac{avx}{b}\right)\right]$.

Set II. When

$$\begin{cases} k_2 = \frac{av+c_3+\sqrt{a^2v^2+2ac_3v+4bvc_3^2}}{2b}, \\ k_1 = 0, \\ b_0 = b_0, \\ a_5 = a_5, \end{cases} \tag{41}$$

by usage of the above values,

$$\Omega_6(x,t) = \frac{2\exp\left[i\left(-vt+\frac{\left(av+c_3+\sqrt{a^2v^2+2ac_3v+4bvc_3^2}\right)x}{2b}\right)\right](-a_3b_1\cos(a_4-a_3vt)sin(a_4-a_3vt)+\Pi_3)}{b_1\cos(a_4-a_3vt)+b_0cosh(a_2-a_1vt)+b_2cosh(a_6-a_5vt)}, \tag{42}$$

where $\Pi_3 = a_1b_0\cosh(a_2-a_1vt)sin(a_4-a_3vt)+a_5b_2cosh(a_2-a_1vt)sinh(a_2-a_1vt)$.

8. HB Approach

We consider f as follows [41]:

$$f = e^{-p(a_2+a_1\zeta)} + b_1e^{p(a_4+a_3\zeta)} + b_0\cos(p_1(a_6+a_5\zeta)), \tag{43}$$

where a_1, a_2, a_3, a_4, b_0, b_1, a_5 and a_6 are constants. Inserting Equation (43) into Equation (37) and selecting coefficients of exp, cos and sin and evaluating them:

Set I. When

$$\begin{cases} c_1 = -\frac{-32a_1^4c_2p^2+3aa_1^2k_1v+aa_1a_3k_1v-2aa_3^2k_1v}{4a_1^2}, \\ k_2 = -\frac{-128a_1^4c_2p^2+3aa_1^2k_1v-3aa_3^2k_1v}{48a_1^3c_5p}, a_5 = 0, \\ c_3 = -\frac{256a_1^7c_2c_5p^5-48aa_1^4a_3c_5k_1p^3v+48aa_1^3a_3^2c_5k_1p^3v-128aa_1^4c_2p^2v+3a_2^2a_1^2k_1v^2-3a^2a_3^2k_1v^2+48a_1^3c_5pv}{-128a_1^4c_2p^2+3aa_1^2k_1v-3aa_3^2k_1v}, \end{cases} \tag{44}$$

via the above values and Equation (6), we obtain

$$\Omega_7(x,t) = \frac{2\left(-a_1e^{-p(a_2+a_1(-vt+k_1x))}p + a_3b_1pe^{-p(a_2+a_1(-vt+k_1x))}\right)e^{i\left(-vt+-\frac{\left(-128a_1^4c_2p^2+3aa_1^2k_1v-3aa_3^2k_1v\right)x}{48a_1^3c_5p}\right)}}{e^{-p(a_2+a_1(-vt+k_1x))}p + b_1pe^{-p(a_2+a_1(-vt+k_1x))} + b_0\cos(a_6p_1)}. \tag{45}$$

Set II. When

$$\begin{cases} c_1 = -\frac{8(9a_1-5a_3)a_1^2c_2p^2}{3a_1-3a_3}, \\ k_1 = -\frac{8}{p^2(a_1-a_3)(a_1-7a_3)a}, \\ v = -\frac{16a_1^4c_2p^4(a_1-7a_3)}{3a_1-3a_3}, a_5 = 0, \\ k_2 = 0. \end{cases} \tag{46}$$

via the above values and Equation (6), we get

$$\Omega_8(x,t) = \frac{2\left(-a_1pe^{-p\left(a_2+a_1\left(\frac{16a_1^4c_2p^4(a_1-7a_3)t}{3a_1-3a_3}--\frac{8x}{p^2(a_1-a_3)(a_1-7a_3)a}\right)\right)} + \Pi_4\right)e^{\frac{16a_1^4c_2p^4(a_1-7a_3)t}{3a_1-3a_3}}}{e^{-p\left(a_2+a_1\left(\frac{16a_1^4c_2p^4(a_1-7a_3)t}{3a_1-3a_3}--\frac{8x}{p^2(a_1-a_3)(a_1-7a_3)a}\right)\right)} + b_0\cos(a_6p_1) + \Pi_5}, \tag{47}$$

where $\Pi_4 = a_1b_1pe^{-p\left(a_2+a_1\left(\frac{16a_1^4c_2p^4(a_1-7a_3)t}{3a_1-3a_3}--\frac{8x}{p^2(a_1-a_3)(a_1-7a_3)a}\right)\right)}$

and $\Pi_5 = b_1e^{p\left(a_2+a_1\left(\frac{16a_1^4c_2p^4(a_1-7a_3)t}{3a_1-3a_3}--\frac{8x}{p^2(a_1-a_3)(a_1-7a_3)a}\right)\right)}$.

9. Evaluation of *M*-Shape Solitons

For this type of solitons, we choose f as [41,42]:

$$f = (d_1\zeta + d_2)^2 + (d_3\zeta + d_4)^2 + d_5, \tag{48}$$

where $d_i(1 \le i \le 5)$ are some constants. Using Equation (20) in Equation (7) and extracting equations from coefficients of ζ and their evaluation gives:

Set I. When $d_2 = d_4 = 0$,

$$\begin{cases} c_1 = -\frac{8c_2\left(d_1^2+d_3^2\right)}{d_5}, v = \frac{c_2d_5\left(d_1^2+d_3^2\right)\left(bc_2d_1^2d_5+bd_3^2d_5-6c_3c_4\right)}{6c_4\left(ac_2d_1^2d_5+acd_3^2d_5+6c_4\right)}, \\ k_1 = 0, \\ k_2 = \frac{c_2d_5\left(d_1^2+d_3^2\right)}{6c_4}. \end{cases} \tag{49}$$

Using the above values we get,

$$\Omega_9(x,t) = \frac{2\left(-\frac{c_2d_1^2\left(d_1^2+d_3^2\right)d_5\left(bc_2d_1^2d_5+bd_3^2d_5-6c_3c_4\right)t}{6c_4\left(ac_2d_1^2d_5+acd_3^2d_5+6c_4\right)} - \frac{c_2d_3^2\left(d_1^2+d_3^2\right)d_5\left(bc_2d_1^2d_5+bd_3^2d_5-6c_3c_4\right)t}{3c_4\left(ac_2d_1^2d_5+acd_3^2d_5+6c_4\right)}\right)N_1}{d_5 + d_1^2\left(\frac{c_2\left(d_1^2+d_3^2\right)d_5\left(bc_2d_1^2d_5+bd_3^2d_5-6c_3c_4\right)t}{6c_4\left(ac_2d_1^2d_5+acd_3^2d_5+6c_4\right)}\right)^2 + d_3^2\left(\frac{c_2\left(d_1^2+d_3^2\right)d_5\left(bc_2d_1^2d_5+bd_3^2d_5-6c_3c_4\right)t}{3c_4\left(ac_2d_1^2d_5+acd_3^2d_5+6c_4\right)}\right)^2}, \tag{50}$$

where $N_1 = \exp\left[i\left(-\frac{c_2\left(d_1^2+d_3^2\right)d_5\left(bc_2d_1^2d_5+bd_3^2d_5-6c_3c_4\right)t}{3c_4\left(ac_2d_1^2d_5+acd_3^2d_5+6c_4\right)} + \frac{c_2d_5\left(d_1^2+d_3^2\right)x}{6c_4}\right)\right]$.

Set II. When $d_4 = d_2 = 0$,

$$\begin{cases} c_1 = -\frac{8c_2\left(d_1^2+d_3^2\right)}{d_5}, \\ v = \frac{c_2d_5\left(d_1^2+d_3^2\right)\left(bc_2d_1^2d_5+bd_3^2d_5-6c_3c_4\right)}{6c_4\left(ac_2d_1^2d_5+acd_3^2d_5+6c_4\right)}, \\ k_1 = \frac{c_2d_5\left(d_1^2+d_3^2\right)a\left(bc_2d_1^2d_5+bd_3^2d_5-6c_3c_4\right)}{6c_4b\left(ac_2d_1^2d_5+acd_3^2d_5+6c_4\right)}, \\ k_2 = \frac{c_2d_5\left(d_1^2+d_3^2\right)}{6c_4}. \end{cases} \tag{51}$$

Using the above values and Equation (6) we get,

$$\Omega_{10}(x,t) = \frac{\left(2\left(2d_1^2\left(-\frac{c_2d_1^2\left(d_1^2+d_3^2\right)d_5\left(bc_2d_1^2d_5+bd_3^2d_5-6c_3c_4\right)t}{6c_4\left(ac_2d_1^2d_5+acd_3^2d_5+6c_4\right)} - \frac{c_2d_3^2\left(d_1^2+d_3^2\right)d_5\left(bc_2d_1^2d_5+bd_3^2d_5-6c_3c_4\right)t}{3c_4\left(ac_2d_1^2d_5+acd_3^2d_5+6c_4\right)}\right)\right)+2\right)N_1}{d_5 + d_1^2\left(\frac{c_2\left(d_1^2+d_3^2\right)d_5\left(bc_2d_1^2d_5+bd_3^2d_5-6c_3c_4\right)t}{6c_4\left(ac_2d_1^2d_5+acd_3^2d_5+6c_4\right)} + \frac{c_2\left(d_1^2+d_3^2\right)d_5\left(bc_2d_1^2d_5+bd_3^2d_5-6c_3c_4\right)x}{3c_4\left(ac_2d_1^2d_5+acd_3^2d_5+6c_4\right)}\right)^2 + N_2^2}, \tag{52}$$

where $N_1 = \exp\left[i\left(-\frac{c_2\left(d_1^2+d_3^2\right)d_5\left(bc_2d_1^2d_5+bd_3^2d_5-6c_3c_4\right)t}{3c_4\left(ac_2d_1^2d_5+acd_3^2d_5+6c_4\right)} + \frac{c_2d_5\left(d_1^2+d_3^2\right)x}{6c_4}\right)\right]$ and,

$N_2 = d_3^2\left(-\frac{c_2\left(d_1^2+d_3^2\right)d_5\left(bc_2d_1^2d_5+bd_3^2d_5-6c_3c_4\right)t}{6c_4\left(ac_2d_1^2d_5+acd_3^2d_5+6c_4\right)} + \frac{ac_2\left(d_1^2+d_3^2\right)d_5\left(bc_2d_1^2d_5+bd_3^2d_5-6c_3c_4\right)x}{6bc_4\left(ac_2d_1^2d_5+acd_3^2d_5+6c_4\right)}\right)$.

10. One-Kink Interaction for *M*-Shape Soliton

We choose f [41,42]:

$$f = \Theta_1^2 + \Theta_2^2 + d_5 + e^{\Theta_3}, \tag{53}$$

the $\Theta_1 = d_1\zeta + d_2, \Theta_2 = d_3\zeta + d_4, \Theta_3 = d_6\zeta + d_7\ d_i(1 \le i \le 7)$, are constants. Applying Equations (53) and (37) and setting equations of ζ and exp coefficients:

Set I. If $d_4 = d_2 = 0$,

$$\begin{cases} c_1 = -\frac{48c_4k_2}{d_5^2}, \\ c_2 = \frac{k_2\left(-c_5^2d_1^2d_5^3-c_5^2d_3^2d_5^2+324c_4^2\right)}{90c_4d_5\left(d_1^2+d_3^2\right)}, \\ v = \frac{ad_3^2d_5^3v^2+192c_4d_1^4+384c_4d_1^2d_3^2+192c_4d_3^4}{d_5^3ad_3^2}, \\ d_6 = \frac{18c_4}{6c_5d_5^2}, k_1 = 0, \\ c_3 = \frac{a_2^2d_3^2d_5^3k_2v_2-abd_3^2d_5^2k_2^2+192ac_4d_1^4k_2+384ac_4d_1^2d_3^2k_2+192ac_4d_3^4k_2+F_1}{d_5^3k_2d_3^2a}, \\ F_1 = ad_3^2d_5^2v_2 + 192c_4d_1^2 + 384c_4d_1^2d_3^2 + 192c_4d_3^4. \end{cases} \tag{54}$$

Using the above values we get,

$$\Omega_{11}(x,t) = \frac{2\left(\frac{18c_4e^{d_7-\frac{18c_4\left(ad_3^2d_5^3v^2+192c_4d_1^4+384c_4d_1^2d_3^2+192c_4d_3^4\right)t}{6c_5d_5^2d_5^3ad_3^2}}}{6c_5d_5^2} - \frac{2t\left(ad_3^2d_5^3v^2+192c_4d_1^4+384c_4d_1^2d_3^2+192c_4d_3^4\right)}{d_5^3a} - H_1\right)H_2}{d_5 + e^{d_7-\frac{18c_4\left(ad_3^2d_5^3v^2+192c_4d_1^4+384c_4d_1^2d_3^2+192c_4d_3^4\right)t}{6c_5d_5^2d_5^3ad_3^2}} + H_3}, \tag{55}$$

where $H_1 = \frac{2d_1^2t\left(ad_3^2d_5^3v^2+192c_4d_1^4+384c_4d_1^2d_3^2+192c_4d_3^4\right)}{d_3^2d_5^3a}$,

$H_2 = \exp\left[i\left(-\frac{t\left(ad_3^2d_5^3v^2+192c_4d_1^4+384c_4d_1^2d_3^2+192c_4d_3^4\right)}{d_3^2d_5^3a} + k_2x\right)\right]$ and

$$H_3 = \frac{d_1^2 t^2 \left(ad_3^2 d_5^3 v^2 + 192c_4 d_1^4 + 384c_4 d_1^2 d_3^2 + 192c_4 d_3^4\right)^2}{d_3^4 d_5^6 a^2} + \frac{t^2 \left(ad_3^2 d_5^3 v^2 + 192c_4 d_1^4 + 384c_4 d_1^2 d_3^2 + 192c_4 d_3^4\right)^2}{d_3^4 d_5^6 a^2}.$$

Set II. When $d_4 = d_2 = 0$,

$$\begin{cases} c_1 = \frac{-16c_5}{4}\left(\frac{-c_5 d_1^4 - 2c_5 d_1^2 d_3^2 - c_5 d_3^4}{81c_4}\right)^{\frac{1}{3}} k_2, \\ c_2 = \frac{c_5 k_2}{30\left(\frac{-c_5 d_1^4 - 2c_5 d_1^2 d_3^2 - c_5 d_3^4}{81c_4}\right)^{\frac{1}{3}}}, \\ d_5 = \frac{d_1^2 + d_3^2}{3\left(\frac{-c_5 d_1^4 - 2c_5 d_1^2 d_3^2 - c_5 d_3^4}{81c_4}\right)^{\frac{1}{3}}}, \\ d_6 = 2\left(\frac{-c_5 d_1^4 - 2c_5 d_1^2 d_3^2 - c_5 d_3^4}{81c_4}\right)^{\frac{1}{3}}. \end{cases} \tag{56}$$

Using the above values we get,

$$\Omega_{12}(x,t) = \frac{2\left(2\left(\frac{-c_5 d_1^4 - 2c_5 d_1^2 d_3^2 - c_5 d_3^4}{81c_4}\right)^{\frac{1}{3}} e^{d_7 + \frac{2\left(\frac{-c_5 d_1^4 - 2c_5 d_1^2 d_3^2 - c_5 d_3^4}{81c_4}\right)^{\frac{1}{3}}(-vt + k_1 x)}{33^{\frac{1}{3}}}} + Q_1\right) e^{i(-vt + k_2 x)}}{\frac{33^{\frac{1}{3}}\left(d_1^2 + d_3^2\right)}{3\left(\frac{-c_5 d_1^4 - 2c_5 d_1^2 d_3^2 - c_5 d_3^4}{81c_4}\right)^{\frac{1}{3}}} + e^{d_7 + \frac{2\left(\frac{-c_5 d_1^4 - 2c_5 d_1^2 d_3^2 - c_5 d_3^4}{81c_4}\right)^{\frac{1}{3}}(-vt + k_1 x)}{33^{\frac{1}{3}}}} + Q_2}, \tag{57}$$

where $Q_1 = 2d_1^2(-vt + k_1 x) + 2d_3^2(-vt + k_1 x)$,

$Q_2 = d_3^2(-vt + k_1 x) + d_3^2(-vt + k_1 x)$.

11. Two-Kink Interaction for *M*-Shape Soliton

We consider [41,42]:

$$f = b_1 e^{-a_1 \zeta + a_2} + b_2 e^{a_3 \zeta + a_4}, \tag{58}$$

where a_1, a_2, a_3 and a_4 are some constants. By usage of Equations (37) and (58) and solving the equations from coefficients of the exp functions:

Set I.

$$\begin{cases} k_1 = \frac{aa_3^2 c_3 + b}{ab(a_3 - 1)(a_3 + 1)a_3^2}, \\ k_2 = \frac{aa_3^2 c_3 + b}{ab(a_3 - 1)(a_3 + 1)}, \\ v = \frac{aa_3^2 c_3 + b}{a^2 (a_3 - 1)(a_3 + 1)a_3^2}, \\ c_1 = 0, a_5 = a_5, a_1 = 0. \end{cases} \tag{59}$$

Using the above values we have,

$$\Omega_{13}(x,t) = \frac{2a_3 b_2 e^{a_4 + a_3\left(-\frac{\left(aa_3^2 c_3 + b\right)t}{ab(a_3 - 1)(a_3 + 1)a_3^2} + \frac{\left(aa_3^2 c_3 + b\right)x}{a(a_3 - 1)(a_3 + 1)a_3^2}\right)} \exp\left[i\left(-\frac{\left(aa_3^2 c_3 + b\right)t}{ab(a_3 - 1)(a_3 + 1)a_3^2} + \frac{\left(aa_3^2 c_3 + b\right)x}{a(a_3 - 1)(a_3 + 1)a_3^2}\right)\right]}{b_1 e^{a_2} + b_2 e^{a_4 + a_3\left(-\frac{\left(aa_3^2 c_3 + b\right)t}{ab(a_3 - 1)(a_3 + 1)a_3^2} + \frac{\left(aa_3^2 c_3 + b\right)x}{a(a_3 - 1)(a_3 + 1)a_3^2}\right)}}. \tag{60}$$

12. Results and Discussion

We have successfully obtained the soliton solutions by assigning appropriate values to parameters and they show a discrepancy of waves. First, by applying the complex envelope ansatz approach, we have evaluated two solution sets for the governing model and their profiles are plotted. Notice that the 3D, 2D and contour grey optical soliton graphs of $\Omega_1(x,t)$ in Equation (18) are presented with distinct parameters $c_2 = 4, \beta = 10, c_3 = 30, c_4 = 5, a = 20, b = 1.4, \lambda = 10, v = 5, \eta = 1$ in Figure 1. Moreover, the black optical soliton graphs of $\Omega_2(x,t)$ in Equation (22) are constructed with distinct parameters $c_2 = 4, c_3 = 30, c_4 = 5, a = 20, b = 1.4, \lambda = 10, v = 5, \eta = 1$ in the 3D, 2D and contour expressions (see Figure 2). Secondly, by applying the complex envelope ansatz approach and Chupin Liu's theorem the combined optical solitons of type-I and type-II are generated. The combined optical soliton type-I graphs of $\Omega_3(x,t)$ in Equation (27) are presented with distinct parameters $c_2 = 4, \beta = 10, c_3 = 30, c_4 = 5, a = 20, b = 1.4, \lambda = 10, v = 5, \eta = 1$ in Figure 3. Similarly, the combined optical soliton type-II profiles for solution $\Omega_4(x,t)$ in Equation (30) are presented with various parameters $c_2 = 4, \beta = 10, c_3 = 30, c_4 = 5, a = 20, b = 1.4, \lambda = 10, v = 5, \eta = 1$ in Figure 4. Furthermore by applying the three-waves assumption on f in Equation (37) we have generated the multiwave solutions respectively. The multiwave graphs of $\Omega_6(x,t)$ in Equation (42) are plotted with distinct parameters $a_3 = 0.25, a_4 = 3, a_1 = 10, a_2 = 1.5, a_5 = 10, a_6 = 3, b_0 = 0.5, c_3 = 3.5, b_1 = 3, b_2 = -2.5, a = 3, b = 1, v = 0.1$ in Figure 5. Moreover, the multiwave graphs of $\Omega_6(x,t)$ in Equation (42) are plotted with distinct parameters $a_3 = 2, a_4 = 1, a_1 = 5, a_2 = 5, a_5 = 4, a_6 = 3, b_0 = 0.5, c_3 = -2, b_1 = -5, b_2 = -2.5, a = 1, b = 1, v = 5$ in Figure 6. Similarly, the multiwave profiles for the solution $\Omega_6(x,t)$ in Equation (42) are plotted via distinct parameters $a_3 = 0.5, a_4 = 7, a_1 = 2, a_2 = 1, a_5 = 4, a_6 = 3, b_0 = 0.5, c_3 = -2, b_1 = -5, b_2 = -2.5, a = 3, b = 1, v = 5$ in Figure 7 respectively. In addition, with the usage of the homoclinic breather (HB) scheme we have computed the 3D, 2D and contour HB graphs of $\Omega_6(x,t)$ in Equation (42). These are plotted with distinct parameters $a_1 = -1, a_3 = 0.25, a_4 = 5, a_6 = 3, b_0 = 0.5, p = 3.5, b_1 = 3, b_2 = -2.5, k_1 = 3, c_2 = 1, c_5 = 3, p_1 = 4, v = 5$ in Figure 8. The 3D, 2D and contour HB profiles of $\Omega_6(x,t)$ in Equation (42) are plotted with distinct parameters $a_1 = -1, a_3 = 3, a_4 = 10, a_6 = 3, b_0 = 0.5, p = 3.5, b_1 = 3, b_2 = -2.5, k_1 = 3, c_2 = 1, c_5 = 3, p_1 = 4, v = 5$ in Figure 9. Furthermore, the HB shapes of $\Omega_6(x,t)$ in Equation (42) are plotted with distinct parameters $a_1 = 0.25, a_3 = 3, a_4 = 10, a_6 = 3, b_0 = 0.5, p = 3.5, b_1 = 3, b_2 = -2.5, k_1 = 3, c_2 = 1, c_5 = 3, p_1 = 4, v = 0.1$ in Figure 10. The 3D M-shape soliton profiles for the solution in Equation (52) are attained with $d_3 = 0.5, d_5 = 5, c_2 = 3, c_3 = 0.5, c_4 = 3.5, d_5 = 3, a = -2.5$ in Figure 11. Similarly, the 2D M-shape soliton profiles for the solution in Equation (52) are computed with $d_3 = 0.5, d_5 = 5, c_2 = 3, c_3 = 0.5, c_4 = 3.5, d_5 = 3, a = -2.5$ in Figure 12. The one-kink M-shape soliton interaction slots via $d_3 = 0.5, c_2 = 3, c_3 = 0.5, c_4 = 3.5, k_1 = 3, k_2 = 1, d_7 = 1, c_5 = 1, v = 1$ are given in Figures 13 and 14 respectively. Finally the 3D M-shape soliton interaction profiles for Equation (60) are plotted with $a_2 = -6, a_4 = 3, b = 0.5, c_3 = 3.5, a = 3, b_1 = 1, b_2 = 4, b = 1$ in Figure 15.

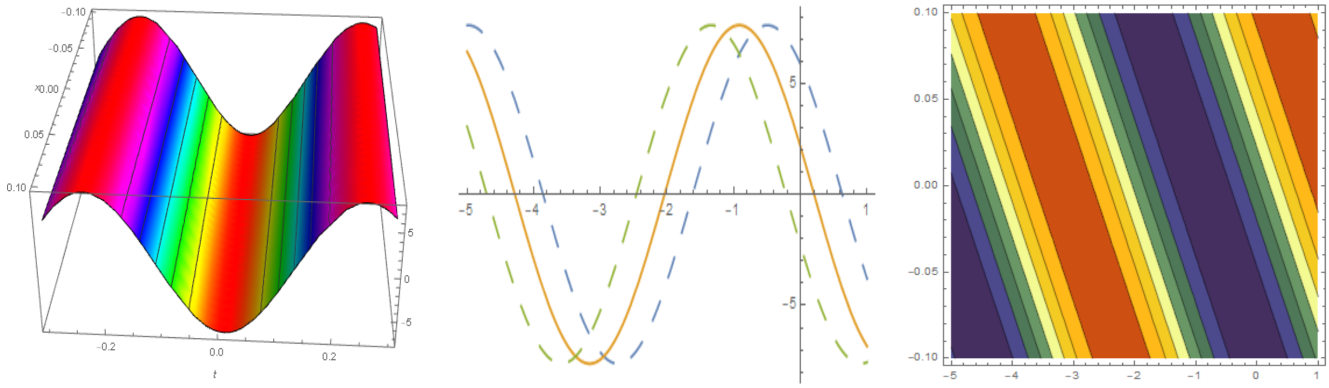

Figure 1. The GOS graphs of $\Omega_1(x,t)$ in Equation (18) are presented via $c_2 = 4, \beta = 10, c_3 = 30$, $c_4 = 5, a = 20, b = 1.4, \lambda = 10, v = 5, \eta = 1$.

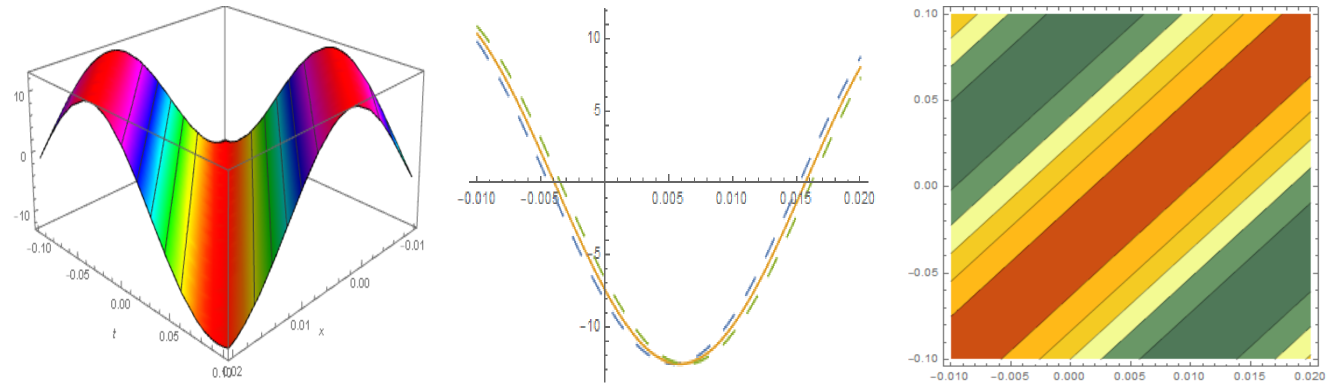

Figure 2. The BOS graphs of $\Omega_2(x,t)$ in Equation (22) are expressed via $c_2 = 4, c_3 = 30, c_4 = 5$, $a = 20, b = 1.4, \lambda = 10, v = 5, \eta = 1$.

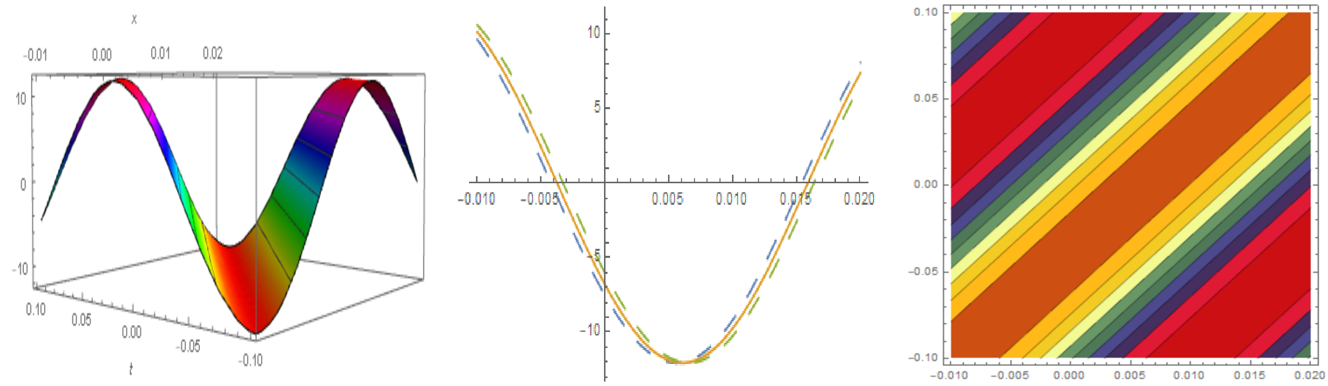

Figure 3. The COS type-I graphs of $\Omega_3(x,t)$ in Equation (27) are presented via $c_2 = 4, \beta = 10$, $c_3 = 30, c_4 = 5, a = 20, b = 1.4, \lambda = 10, v = 5, \eta = 1$.

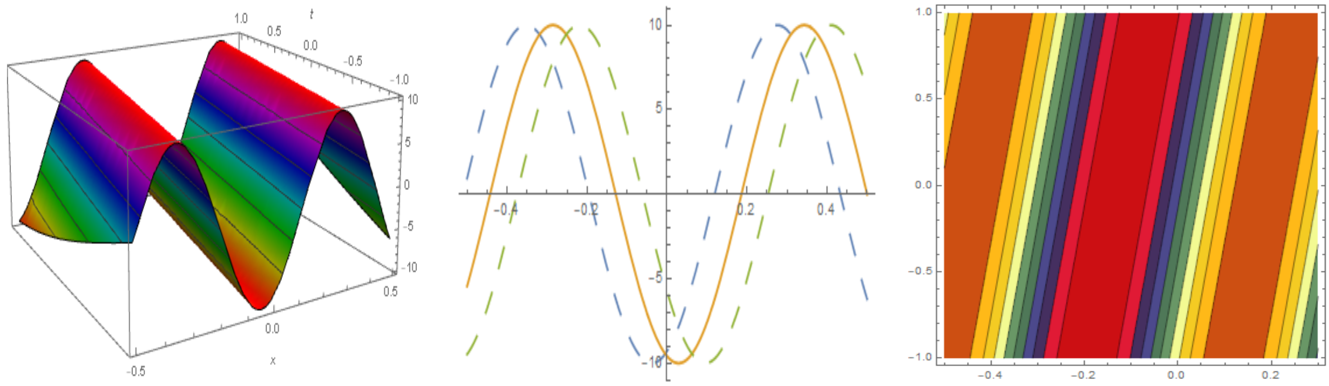

Figure 4. The COS type-II graphs of $\Omega_4(x,t)$ in Equation (30) are plotted via $c_2 = 4, \beta = 10, c_3 = 30, c_4 = 5, a = 20, b = 1.4, \lambda = 10, v = 5, \eta = 1$.

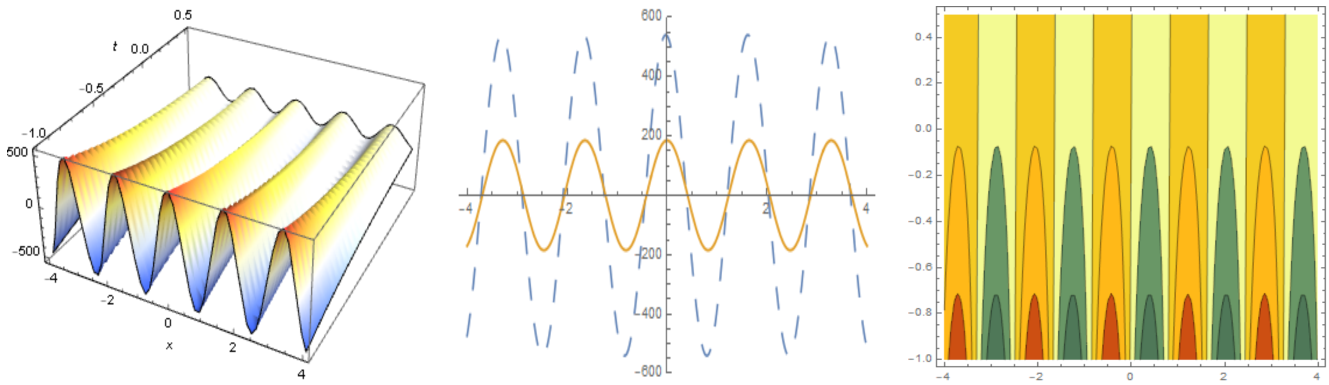

Figure 5. The multiwave graphs of $\Omega_6(x,t)$ in Equation (42) are plotted with $a_3 = 0.25$, $a_4 = 3$, $a_1 = 10$, $a_2 = 1.5$, $a_5 = 10$, $a_6 = 3$, $b_0 = 0.5$, $c_3 = 3.5$, $b_1 = 3$, $b_2 = -2.5$, $a = 3$, $b = 1$, $v = 0.1$.

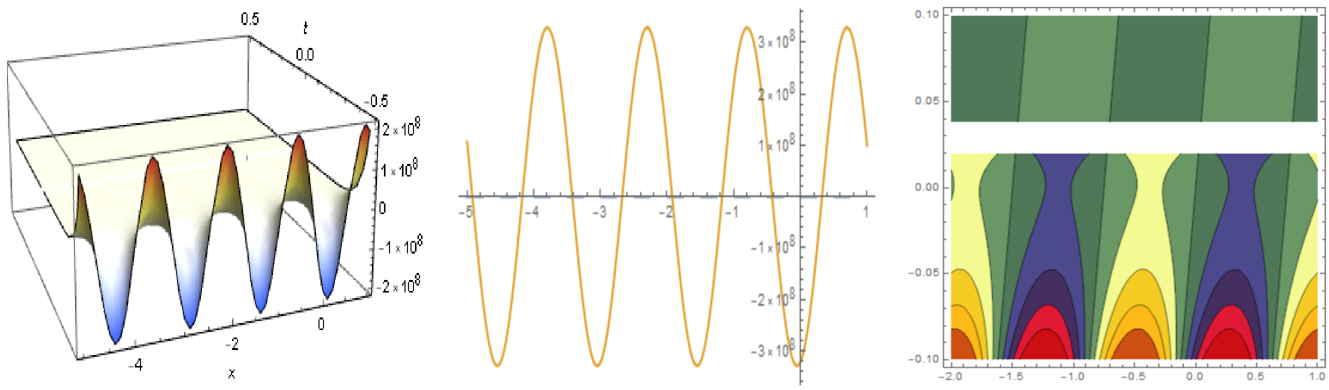

Figure 6. The multiwave graphs of $\Omega_6(x,t)$ in Equation (42) are plotted with $a_3 = 2$, $a_4 = 1$, $a_1 = 5$, $a_2 = 5$, $a_5 = 4$, $a_6 = 3$, $b_0 = 0.5$, $c_3 = -2$, $b_1 = -5$, $b_2 = -2.5$, $a = 1$, $b = 1$, $v = 5$.

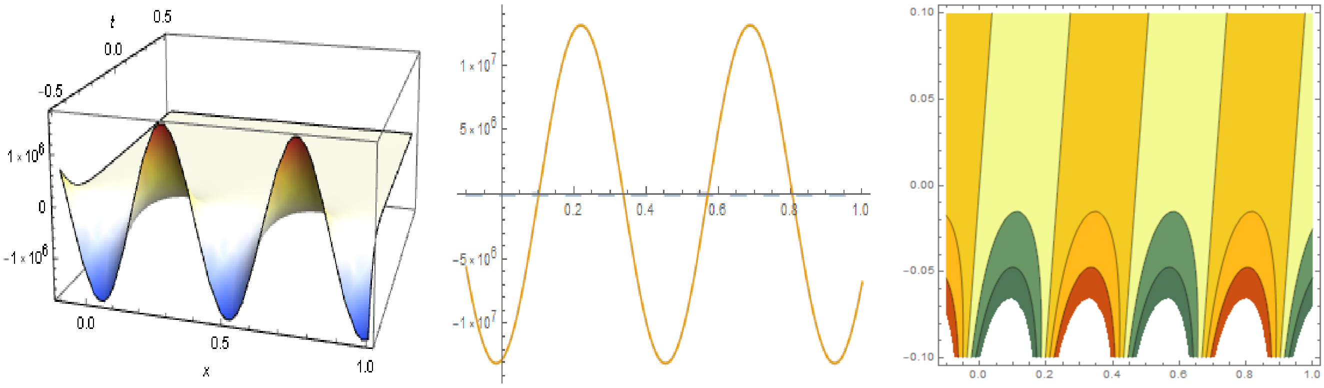

Figure 7. The multiwave graphs of $\Omega_6(x,t)$ in Equation (42) are plotted with $a_3 = 0.5$, $a_4 = 7$, $a_1 = 2$, $a_2 = 1$, $a_5 = 4$, $a_6 = 3$, $b_0 = 0.5$, $c_3 = -2$, $b_1 = -5$, $b_2 = -2.5$, $a = 3$, $b = 1$, $v = 5$.

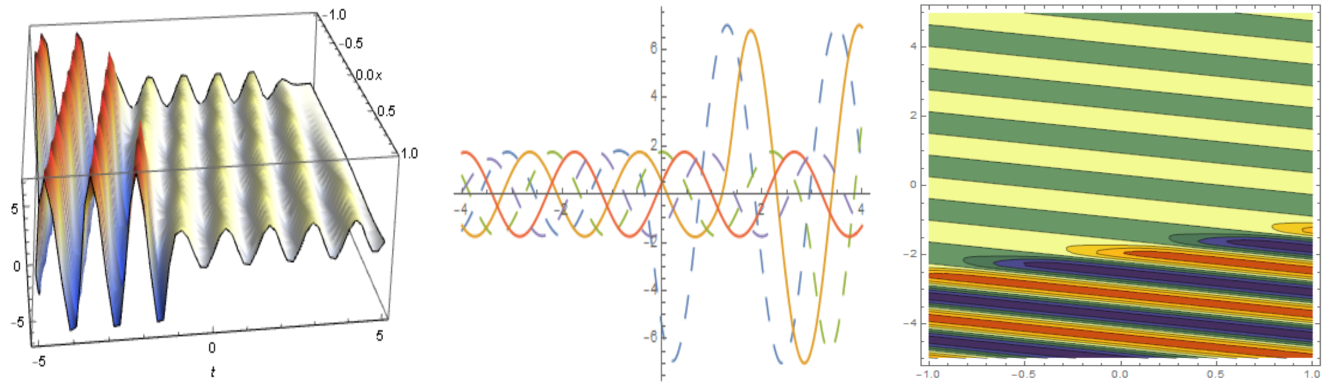

Figure 8. The 3D, 2D and contour HB graphs of $\Omega_6(x,t)$ in Equation (42) are plotted with distinct parameters $a_1 = -1$, $a_3 = 0.25$, $a_4 = 5$, $a_6 = 3$, $b_0 = 0.5, p = 3.5$, $b_1 = 3$, $b_2 = -2.5$, $k_1 = 3$, $c_2 = 1$, $c_5 = 3, p_1 = 4$, $v = 5$, respectively.

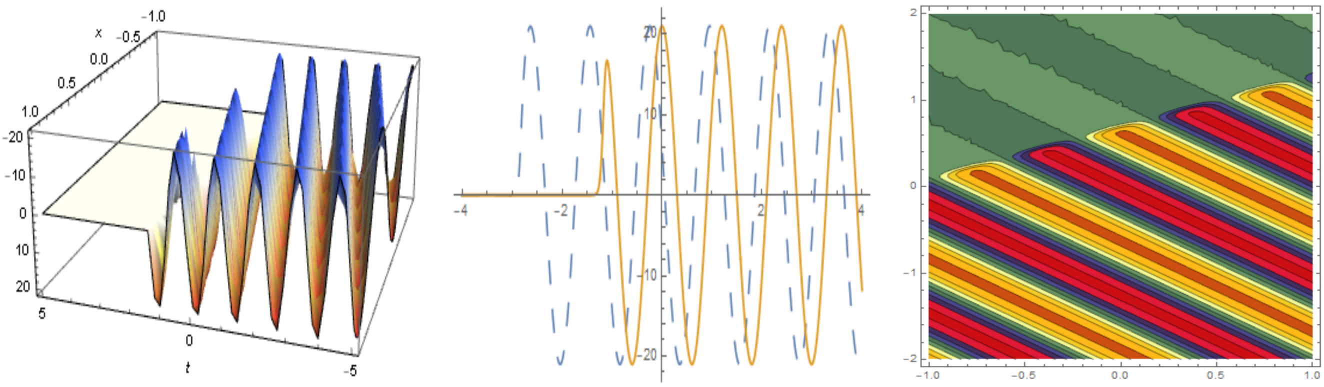

Figure 9. The 3D, 2D and contour HB profiles of $\Omega_6(x,t)$ in Equation (42) are plotted with distinct parameters $a_1 = -1$, $a_3 = 3$, $a_4 = 10$, $a_6 = 3$, $b_0 = 0.5$, $p = 3.5$, $b_1 = 3$, $b_2 = -2.5$, $k_1 = 3$, $c_2 = 1$, $c_5 = 3$, $p_1 = 4$, $v = 5$, respectively.

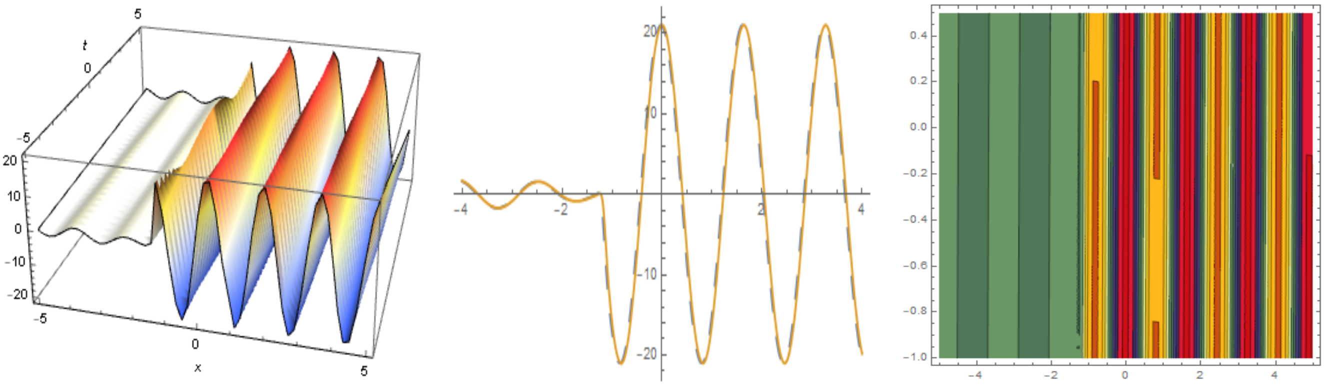

Figure 10. The 3D, 2D and contour HB shapes of $\Omega_6(x,t)$ in Equation (42) are plotted with distinct parameters $a_1 = 0.25,\ a_3 = 3,\ a_4 = 10,\ a_6 = 3,\ b_0 = 0.5,\ p = 3.5,\ b_1 = 3,\ b_2 = -2.5,\ k_1 = 3,\ c_2 = 1,$ $c_5 = 3,\ p_1 = 4,\ v = 0.1$, respectively.

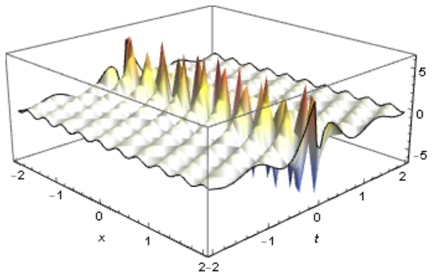

(**a**) $d_1 = -6$

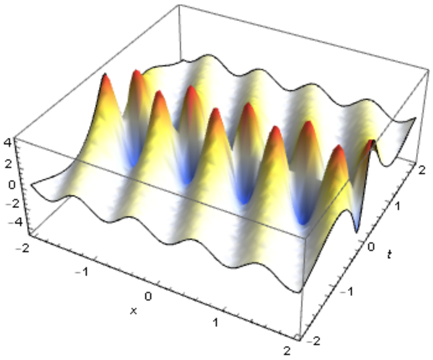

(**b**) $d_1 = -4$

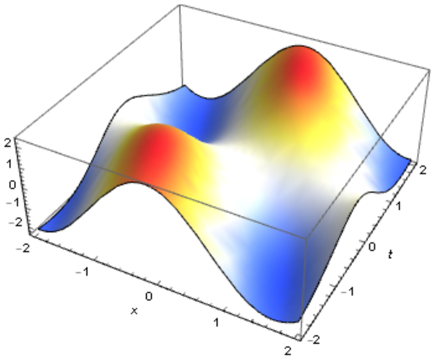

(**c**) $d_1 = -2$

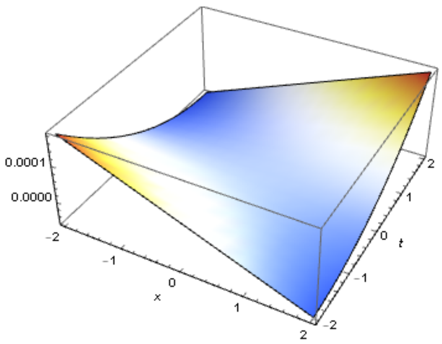

(**d**) $d_1 = 0$

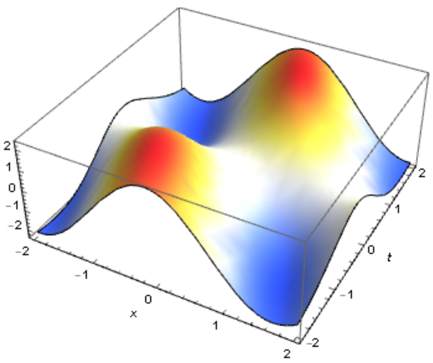

(**e**) $d_1 = 2$

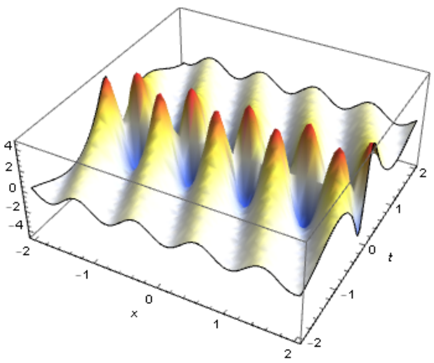

(**f**) $d_1 = 4$

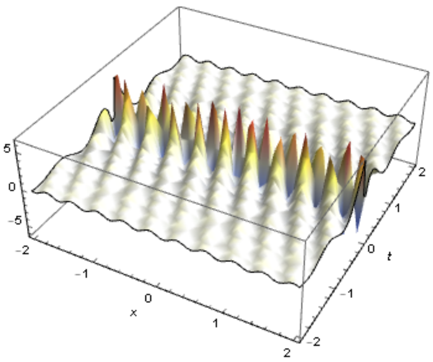

(**g**) $d_1 = 6$

Figure 11. The 3D *M*-shape soliton profiles for the solution in Equation (52) are constructed with $d_3 = 0.5,\ d_5 = 5,\ c_2 = 3,\ c_3 = 0.5,\ c_4 = 3.5,\ d_5 = 3,\ a = -2.5$.

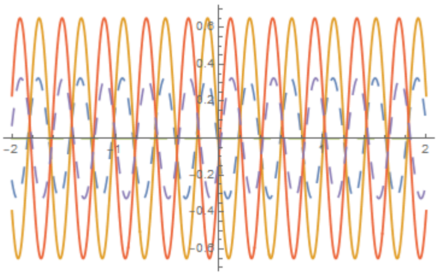

(**a**) $d_1 = -6$

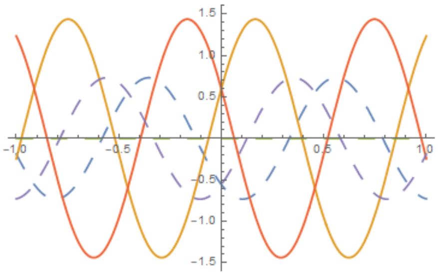

(**b**) $d_1 = -4$

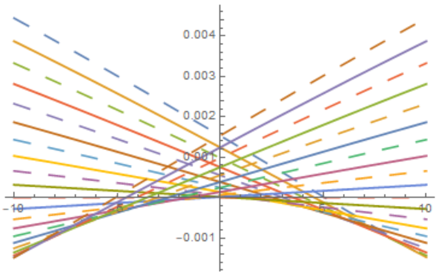

(**c**) $d_1 = -2$

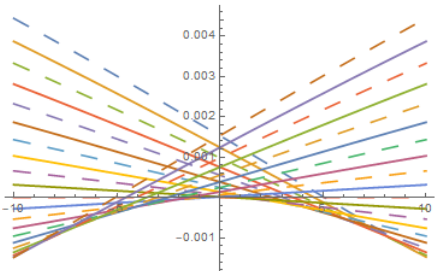

(**d**) $d_1 = 0$

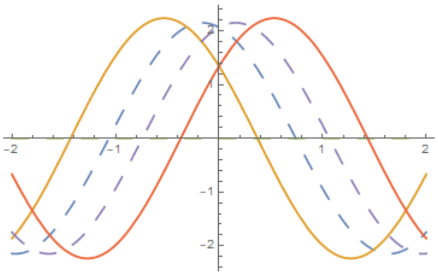

(**e**) $d_1 = 2$

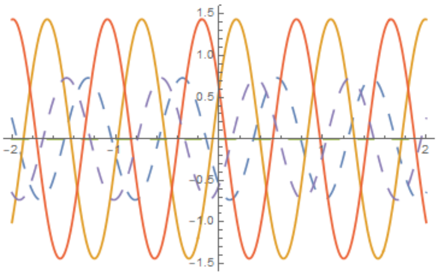

(**f**) $d_1 = 4$

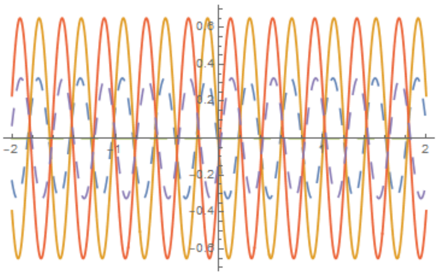

(**g**) $d_1 = 6$

Figure 12. The 2D *M*-shape soliton profiles for the solution in Equation (52) are constructed with $d_3 = 0.5,\ d_5 = 5,\ c_2 = 3,\ c_3 = 0.5,\ c_4 = 3.5,\ d_5 = 3,\ a = -2.5$.

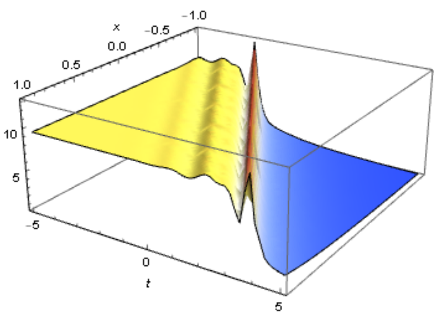

(**a**) $d_1 = -6$

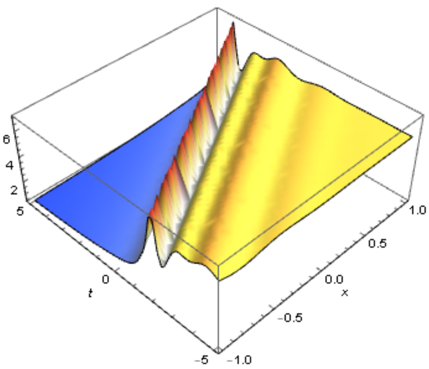

(**b**) $d_1 = -4$

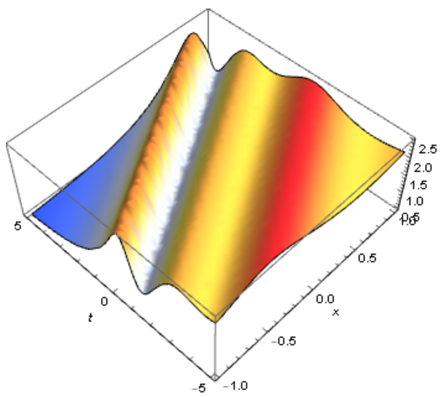

(**c**) $d_1 = -2$

Figure 13. *Cont.*

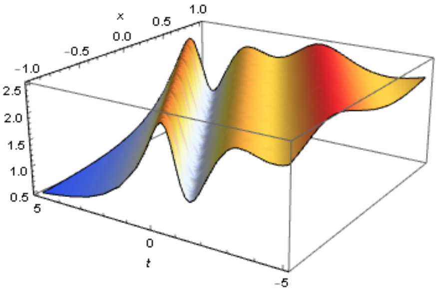

(**d**) $d_1 = 0$

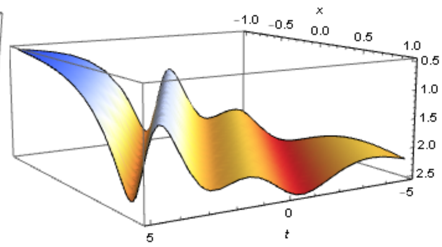

(**e**) $d_1 = 2$

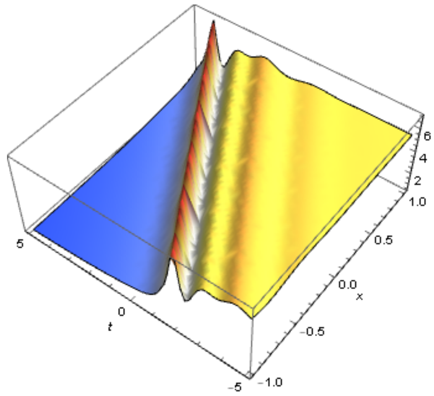

(**f**) $d_1 = 4$

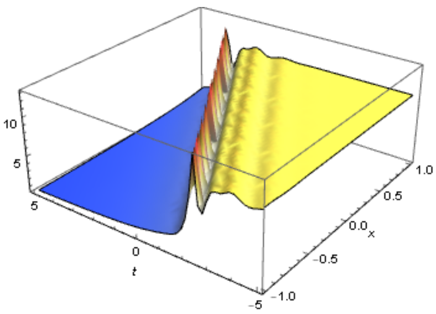

(**g**) $d_1 = 6$

Figure 13. One-kink interaction for M-shape soliton to Equation (57) via $d_3 = 0.5, c_2 = 3, c_3 = 0.5, c_4 = 3.5, k_1 = 3, k_2 = 1, d_7 = 1, c_5 = 1, v = 1$.

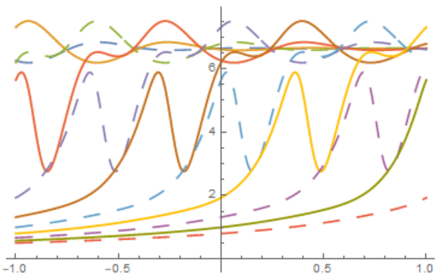

(**a**) $d_1 = -6$

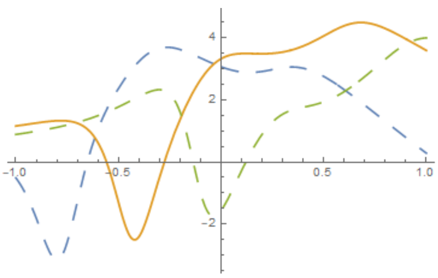

(**b**) $d_1 = -4$

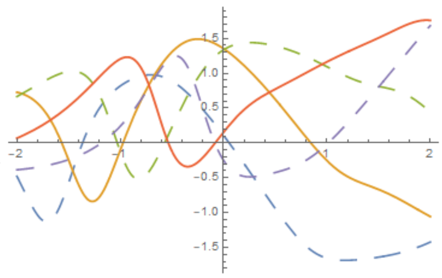

(**c**) $d_1 = -2$

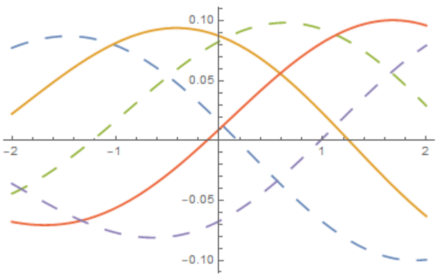

(**d**) $d_1 = 0$

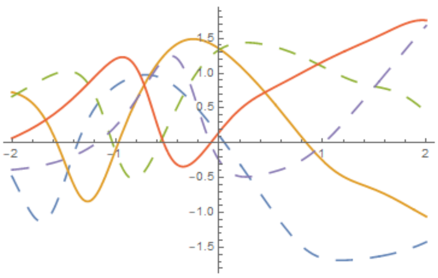

(**e**) $d_1 = 2$

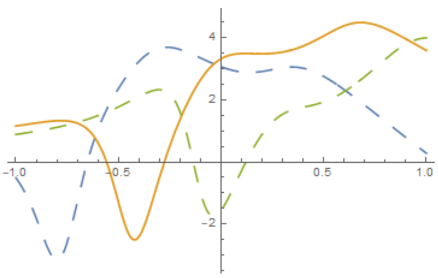

(**f**) $d_1 = 4$

Figure 14. *Cont.*

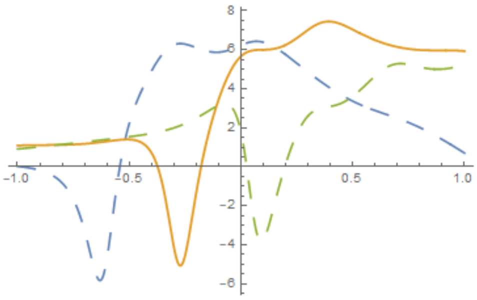

(**g**) $d_1 = 6$

Figure 14. The 2D profiles for Figure 13, respectively.

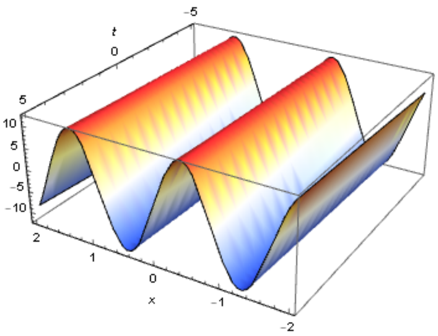

(**a**) $a_3 = -6$

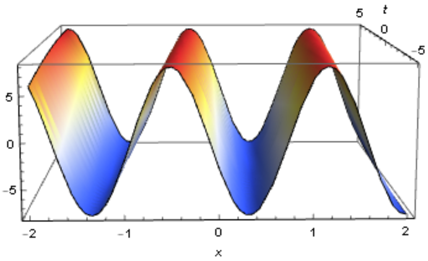

(**b**) $a_3 = -4$

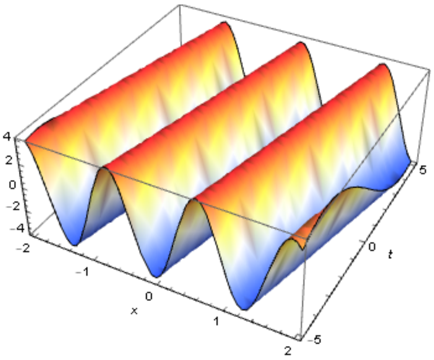

(**c**) $a_3 = -2$

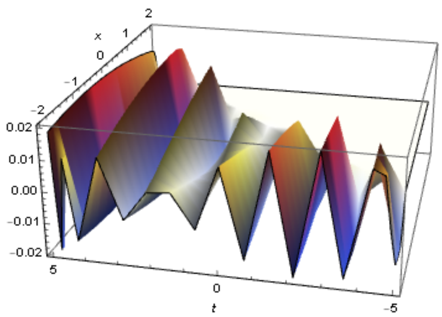

(**d**) $a_3 = 0.02$

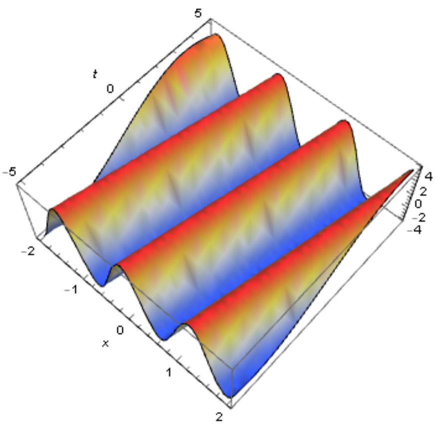

(**e**) $a_3 = 2$

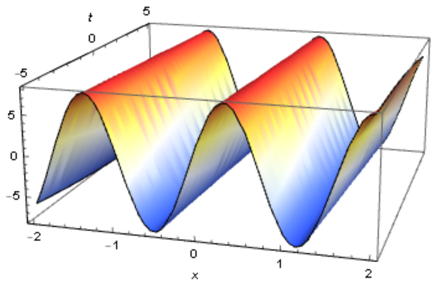

(**f**) $a_3 = 4$

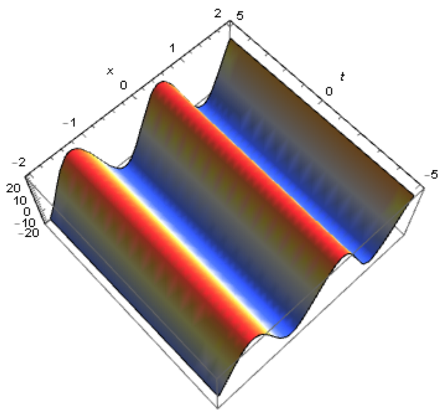

(**g**) $a_3 = 10$

Figure 15. The 3D *M*-shape soliton interaction profiles for the solution in Equation (60) are constructed with $a_2 = -6,\ a_4 = 3,\ b = 0.5,\ c_3 = 3.5,\ a = 3,\ b_1 = 1,\ b_2 = 4,\ b = 1$.

13. Conclusions

This article derived the grey and black optical solitons to the IP-NLSE with and dual power law nonlinearity via a complex envelope ansatz solution which arises in optical fibers and photovoltaic-photo-refractive materials. We thereafter applied the CLT to compute new forms of COS. Furthermore, the propagation of homoclinic breathers, multiwaves and M-shape solitons is analytically deliberated. All new analytical solutions are evaluated by ansatz functions techniques and transformation involving logarithmic functions. Multiwave solitons are successfully constructed by using the three-waves method. Two categories of interactions for M-shape solitons through exponential functions are successfully examined in Figures 13–15.

Author Contributions: Methodology, S.T.R.R.; Formal analysis, S.A.M.A.; Supervision, A.R.S. All authors have read and agreed to the published version of the manuscript.

Funding: This research received no external funding.

Data Availability Statement: Not applicable.

Acknowledgments: The authors extend their appreciation to the Deanship for Research and Innovation, Ministry of Education in Saudi Arabia for funding this research work through the project number: IFP22UQU4290491DSR141.

Conflicts of Interest: The authors declare no conflict of interest.

References

1. Baldelli, L.; Filippucci, R. Singular quasilinear critical Schrodinger equations in RN. *Commun. Pure Appl. Anal.* **2022**, *21*, 2561–2586. [CrossRef]
2. Filippucci, R.; Pucci, P.; Souplet, P. A Liouville-type theorem in a half-space and its applications to the gradient blow-up behavior for superquadratic diffusive Hamilton-Jacobi equations. *Comm. Partial. Differ. Equations* **2020**, *45*, 321–349. [CrossRef]
3. Seadawy, A.R.; Ahmed, S.; Rizvi, S.T.; Nazar, K. Applications for mixed Chen–Lee–Liu derivative nonlinear Schrödinger equation in water wave flumes and optical fibers. *Optical Quantum Electron.* **2023**, *55*, 34. [CrossRef]
4. Seadawy, A.R.; Rizvi, S.T.; Ahmed, S.; Ahmad, A. Study of dissipative NLSE for dark and bright, multiwave, breather and *M*-shaped solitons along with some interactions in monochromatic waves. *Opt. Quantum Electron.* **2022**, *54*, 782. [CrossRef]
5. Ahmed, S.; Seadawy, A.R.; Rizvi, S.T. Study of breathers, rogue waves and lump solutions for the nonlinear chains of atoms. *Opt. Quantum Electron.* **2022**, *54*, 320. [CrossRef]
6. Ali, K.; Seadawy, A.R.; Ahmed, S.; Rizvi, S.T. Discussion on rational solutions for Nematicons in liquid crystals with Kerr Law. *Chaos Solitons Fractals* **2022**, *160*, 112218. [CrossRef]
7. Seadawy, A.R.; Rizvi, S.T.; Ahmed, S. Weierstrass and Jacobi elliptic, bell and kink type, lumps, Ma and Kuznetsov breathers with rogue wave solutions to the dissipative nonlinear Schrödinger equation. *Chaos Solitons Fractals* **2022**, *160*, 112258. [CrossRef]
8. Khater, A.H.; Obied Allah, M.H. Effects of rotation on Rayleigh-Taylor instabilities of an accelerating, compressible, perfectly conducting plane layer. *Astrophys. Space Sci.* **1984**, *106*, 245–255. [CrossRef]
9. Helal, M.A. A Chebyshev spectral method for solving Korteweg–de Vries equation with hydrodynamical application. *Chaos Solitons Fractals* **2001**, *12*, 943–950. [CrossRef]
10. Helal, M.A.; Mehanna, M.S. A comparative study between two different methods for solving the general Korteweg–de Vries Equation (GKdV). *Chaos Solitons Fractals* **2007**, *33*, 725–739. [CrossRef]
11. Seadawy, A.R.; Cheemaa, N. Propagation of nonlinear complex waves for the coupled nonlinear Schrödinger Equations in two core optical fibers. *Phys. A Stat. Mech. Appl.* **2019**, *529*, 121330. [CrossRef]
12. Ghaffar, A.; Ali, A.; Ahmed, S.; Akram, S.; Baleanu, D.; Nisar, K.S. A novel analytical technique to obtain the solitary solutions for nonlinear evolution equation of fractional order. *Adv. Differ. Equ.* **2020**, *2020*, 308. [CrossRef]
13. Wazwaz, A.M. Higher dimensional nonlinear Schrödinger equations in anomalous dispersion and normal dispersive regimes: Bright and dark optical solitons. *Optik* **2020**, *222*, 165327. [CrossRef]
14. Cheemaa, N.; Seadawy, A.R.; Chen, S. More general families of exact solitary wave solutions of the nonlinear Schrodinger equation with their applications in nonlinear optics. *Eur. Phys. J. Plus* **2018**, *133*, 547. [CrossRef]
15. Arshad, M.; Seadawy, A.; Lu, D.; Wang, J. Travelling wave solutions of generalized coupled Zakharov–Kuznetsov and dispersive long wave equations. *Results Phys.* **2016**, *6*, 1136–1145. [CrossRef]
16. Helal, M.A. *Solitons, A Volume in the Encyclopedia of Complexity and Systems Science*, 2nd ed.; Springer Science: Berlin, Germany, 2022.
17. Seadawy A.R. Stability analysis of traveling wave solutions for generalized coupled nonlinear KdV equations. *Appl. Math. Inf. Sci.* **2016**, *10*, 209–214. [CrossRef]
18. Seadawy, A.R.; Iqbal, M.; Lu, D. Application of mathematical methods on the ion sound and Langmuir waves dynamical systems. *Praman-J. Phys.* **2019**, *93*, 10. [CrossRef]

19. Liu, Y.; Li, B.; Wazwaz, A.M. Novel high-order breathers and rogue waves in the Boussinesq equation via determinants. *Int. J. Mod. Phys. B* **2020**, *43*, 3701–3715. [CrossRef]
20. Shah, K.; Seadawy, A.R.; Arfan, M. Evaluation of one dimensional fuzzy fractional partial differential equations. *Alex. Eng. J.* **2020**, *59*, 3347–3353. [CrossRef]
21. Wang, J.; Shehzad, K.; Seadawy, A.R. Muhammad Arshad and Farwa Asmat, Dynamic study of multi-peak solitons and other wave solutions of new coupled KdV and new coupled Zakharov–Kuznetsov systems with their stability. *J. Taibah Univ. Sci.* **2023**, *17*, 2163872. [CrossRef]
22. Wazwaz, A.M.; Mehanna, M. Bright and dark optical solitons for a new (3+ 1)-dimensional nonlinear Schrödinger equation. *Optik* **2021**, *241*, 166985. [CrossRef]
23. Triki, H.; Biswas, A.; Milovic, D.; Belic, M. Chirped femtosecond pulses in the higher-order nonlinear Schrödinger equation with non-Kerr nonlinear terms and cubic–quintic–septic nonlinearities. *Opt. Commun.* **2016**, *366*, 362–369. [CrossRef]
24. Taghizadeh, N.; Mirzazadeh, M.; Farahrooz, F. Exact solutions of the nonlinear Schrödinger equation by the first integral method. *J. Math. Anal. Appl.* **2011**, *374*, 549–553. [CrossRef]
25. Seadawy, A.R. The generalized nonlinear higher order of KdV equations from the higher order nonlinear Schrödinger equation and its solutions. *Optik* **2017**, *139*, 31–34. [CrossRef]
26. Chen, J.; Luan, Z.; Zhou, Q.; Alzahrani, A.K.; Biswas, A.; Liu, W. Periodic soliton interactions for higher-order nonlinear Schrödinger equation in optical fibers. *Nonlinear Dyn.* **2020**, *100*, 2817–2821. [CrossRef]
27. Savaissou, N.; Gambo, B.; Rezazadeh, H.; Bekir, A.; Doka, S.Y. Exact optical solitons to the perturbed nonlinear Schrödinger equation with dual-power law of nonlinearity. *Opt. Quantum Electron.* **2020**, *52*, 318. [CrossRef]
28. Kudryashov, N.A. Almost general solution of the reduced higher-order nonlinear Schrödinger equation. *Optik* **2021**, *230*, 166347. [CrossRef]
29. Kudryashov, N.A. Optical solitons of the resonant nonlinear Schrödinger equation with arbitrary index. *Optik* **2021**, *235*, 166626. [CrossRef]
30. Ma, G.; Zhao, J.; Zhou, Q.; Biswas, A.; Liu, W. Soliton interaction control through dispersion and nonlinear effects for the fifth-order nonlinear Schrödinger equation. *Nonlinear Dyn.* **2021**, *106*, 2479–2484. [CrossRef]
31. Wang, K.J.; Wang, G.D. Variational theory and new abundant solutions to the (1+ 2)-dimensional chiral nonlinear Schrödinger equation in optics. *Phys. Lett. A* **2021**, *412*, 127588. [CrossRef]
32. Mo, Y.; Ling, L.; Zeng, D. Data-driven vector soliton solutions of coupled nonlinear Schrödinger equation using a deep learning algorithm. *Phys. Lett. A* **2022**, *421*, 127739. [CrossRef]
33. Jiang, C.; Cui, J.; Qian, X.; Song, S. High-order linearly implicit structure-preserving exponential integrators for the nonlinear Schrödinger equation. *J. Sci. Comput.* **2022**, *90*, 66. [CrossRef]
34. Weng, W.; Zhang, G.; Zhang, M.; Zhou, Z.; Yan, Z. Semi-rational vector rogon-soliton solutions and asymptotic analysis for any n-component nonlinear Schrödinger equation with mixed boundary conditions. *Phys. D Nonlinear Phenom.* **2022**, *432*, 133150. [CrossRef]
35. Biswas, A.; Ekici, M.; Sonmezoglu, A.; Arshed, S.; Belic, M. Optical soliton perturbation with full nonlinearity by extended trial function method. *Opt. Quantum Electron.* **2017**, *44*, 125–138. [CrossRef]
36. Ekici, M.; Sonmezoglu, A.; Zhou, Q.; Moshokoa, S.P.; Ullah, M.Z.; Arnous, A.H.; Belic, M. Analysis of optical solitons in nonlinear negative-indexed materials with anti-cubic nonlinearity. *Opt. Quantum Electron.* **2019**, *53*, 715. [CrossRef]
37. Seadawy, A.R.; Rizvi, S.T.; Ashraf, M.A.; Younis, M.; Hanif, M. Rational solutions and their interactions with kink and periodic waves for a nonlinear dynamical phenomenon. *Int. J. Mod. Phys. B* **2021**, *35*, 2150236. [CrossRef]
38. Manafian, J.; Mohammadi Ivatloo, B.; Abapour, M. Breather wave, periodic, and cross-kink solutions to the generalized Bogoyavlensky-Konopelchenko equation. *Math. Methods Appl. Sci.* **2020**, *43*, 1753–1774. [CrossRef]
39. Alsallami, S.A.M.; Rizvi, S.T.R.; Seadawy, A.R. Study of Stochastic–Fractional Drinfel'd–Sokolov–Wilson Equation for *M*-shaped Rational, Homoclinic Breather, Periodic and Kink-Cross Rational Solutions. *Mathematics* **2023**, *11*, 1504. [CrossRef]
40. Aliyu, A.I.; Tchier, F.; Inc, M.; Yusuf, A.; Baleanu, D. Dynamics of optical solitons, multipliers and conservation laws to the nonlinear Schrödinger equation in (2+1)-dimensions with non-Kerr law nonlinearity. *J. Mod. Opt.* **2019**, *1950*, 1162–1174. [CrossRef]
41. Ahmed, I.; Seadawy, A.R.; Lu, D. Kinky breathers, W-shaped and multi-peak solitons interaction in $(2+1)$-dimensional nonlinear Schrödinger equation with Kerr law of nonlinearity. *Eur. Phys. J. Plus* **2019**, *134*, 1–10. [CrossRef]
42. Ahmed, I.; ASeadawy, R.; Lu, D. *M*-shaped rational solitons and their interaction with kink waves in the Fokas–Lenells equation. *Phys. Scr.* **2019**, *94*, 055205. [CrossRef]